A Learning-Based Nonlinear Elimination Technique for Parameterized Incompressible Navier-Stokes Equations

Yingzhi Liu[0000−0001−9962−7310], Fenfen Qi[0009−0004−5343−8839], and Xiao-Chuan Cai[0000−0003−0296−8640]

1 Introduction

Numerical simulation of blood flow has many important applications in hemodynamics and biomedical engineering. For instance, one can predict the risk and provide assessment of certain vascular diseases [3]. For modeling the patient-specific blood flow, the unsteady incompressible Navier-Stokes equations with individualized boundary conditions can be used. As is well-known the behavior of blood flow can be very different in different scenarios that are characterized by different parameters of the Navier-Stokes equations [10]. Most numerical simulations [4, 6, 9] focuses on a single set of the parameters. A systematic study for all possible scenarios would be useful, but computationally extremely expensive. In this paper, we focus on the numerical simulation of blood flows in different scenarios and introduce a learning-based nonlinear elimination method to improve the convergence of the inexact Newton method. Each scenario is determined by a set of six parameters, and a training step is performed using several scenarios, then some components of trained problem are used to accelerate the simulation of other scenarios. For problems in abnormal arteries, the traditional inexact Newton method is usually difficult to converge [8]. Extending the method in [7] for three-dimensional patient-specific parametrized blood flow problems, we investigate a nonlinear elimination preconditioned inexact Newton method with backtracking (INB-NE) in which we include a learning step that trains the solver from a specific set of the parameters. Once the method is trained for an especially difficult situation, it can be applied to other scenarios with much improved convergence compared with the classical method that always start from scratch. Different from the previous INB-NE methods [8, 2, 5, 11], the learning-based method constructs the subspaces of the strong nonlinear residuals and the corresponding variables by a principal component analysis that is able to cap-

Yingzhi Liu, Fenfen Qi, and Xiao-Chuan Cai
Department of Mathematics, University of Macau, Macau,
e-mail: {yingzhiliu,yc27956,xccai}@um.edu.mo

ture the location where the large nonlinear residual occurs by eliminating these large residuals. Fast convergence of the proposed method is realized for many parameter combinations necessary for the diagnosis of the diseases.

2 Model problem and its discretization

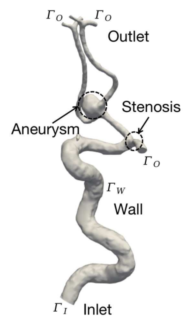

Fig. 1 An abnormal artery with stenosis and aneurysm.

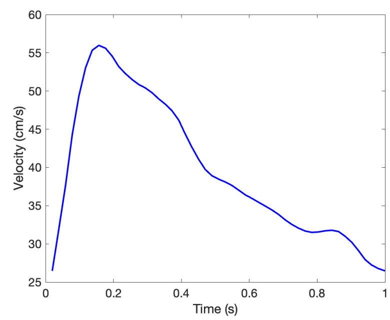

Fig. 2 The clinically measured inflow velocity profile in a cardiac cycle.

Denote by $\Omega \subset \mathbb{R}^3$ an artery with Γ_I, Γ_W and Γ_O the inlet, wall and outlets, respectively, see, for example, the left of Fig. 1 for an artery with a stenosis and aneurysm. In Ω, we consider the unsteady incompressible Navier-Stokes equations

$$\begin{cases} \rho\left(\frac{\partial \boldsymbol{u}}{\partial t} + \boldsymbol{u}\cdot\nabla\boldsymbol{u}\right) - \mu\Delta\boldsymbol{u} + \nabla p = \boldsymbol{0} \text{ in } \Omega\times(0,T), \\ \nabla\cdot\boldsymbol{u} = 0 \text{ in } \Omega\times(0,T), \\ \boldsymbol{u}(\boldsymbol{x},0) = \boldsymbol{0} \text{ in } \Omega\times\{0\}, \end{cases} \tag{1}$$

where $\boldsymbol{u}$ and p are the velocity and pressure, respectively. For the patient-specific simulation of blood flows, on the boundary $\partial\Omega = \Gamma_I \cup \Gamma_W \cup \Gamma_O$, we adopt the following boundary conditions

$$\begin{array}{ll} \boldsymbol{u} = \boldsymbol{u}_I & \text{on } \Gamma_I, \\ \boldsymbol{u} = \boldsymbol{0} & \text{on } \Gamma_W, \\ p = R_i Q_i & \text{on } \Gamma_O^i,\ i = 1,\ldots,m \end{array} \tag{2}$$

where $\boldsymbol{u}_I$ is the clinically measured inlet velocity, R_i is the resistance and Q_i is the fluid flux. In general, the model depends on the viscosity μ (g/(cm·s)), density ρ (g/cm^2), inlet velocity $\boldsymbol{u}_I$ and the resistance R_i. Since $\boldsymbol{u}_I$ and R_i can be determined by the systolic velocity u_S (cm/s), the heart rate r_C (BPM), the systolic pressure (p_S (mmHg) and the diastolic pressure p_D (mmHg), in the rest of paper, we use

$$\text{Pat} = \{\mu, \rho, u_S, r_C, p_S, p_D\},$$

to denote the set of "Pat"ient-specific parameters. Denote $(\cdot,\cdot)_K$, $(\cdot,\cdot)$ and $\langle\cdot,\cdot\rangle_{\Gamma_O}$ as the inner product in $L^2(K)$, $L^2(\Omega)$ and $L^2(\Gamma_O)$, respectively. We use a stabilized P1-P1 finite element method to obtain the semi-discretized form of the 3D Navier-Stokes equations

$$\begin{cases} \left(\rho\dfrac{\partial \boldsymbol{u}_h}{\partial t}, \boldsymbol{v}_h\right) + (\mu\nabla\boldsymbol{u}_h, \nabla\boldsymbol{v}_h) - (p_h, \nabla\cdot\boldsymbol{v}_h) + (q_h, \nabla\cdot\boldsymbol{u}_h) + (\rho\boldsymbol{u}_h\cdot\nabla\boldsymbol{u}_h, \boldsymbol{v}_h) \\ \quad - \langle\mu\nabla\boldsymbol{u}_h\cdot\boldsymbol{n}, \boldsymbol{v}_h\rangle_{\Gamma_O} + \displaystyle\sum_{i=1}^{m} R_i \int_{\Gamma_O^i} \boldsymbol{u}_h\cdot\boldsymbol{n}\,\mathrm{d}\Gamma_O^i \int_{\Gamma_O^i} \boldsymbol{v}_h\cdot\boldsymbol{n}\,\mathrm{d}\Gamma_O^i \\ \quad + \displaystyle\sum_{K\in\mathcal{T}_h} \left(\rho\left(\dfrac{\partial\boldsymbol{u}_h}{\partial t} + \boldsymbol{u}_h\cdot\nabla\boldsymbol{u}_h\right) + \nabla p_h, \gamma_1(\boldsymbol{u}_h\cdot\nabla\boldsymbol{v}_h + \nabla q_h)\right)_K \\ \quad + \displaystyle\sum_{K\in\mathcal{T}_h} (\nabla\cdot\boldsymbol{u}_h, \gamma_2\nabla\cdot\boldsymbol{v}_h)_K = 0, \end{cases} \tag{3}$$

for any $\boldsymbol{v_h}$ and q_h in the corresponding finite element spaces, respectively, where γ_1 and γ_2 are stabilization parameters [4]. For the temporal discretization, the second-order backward differentiation formula (BDF2) with a fixed time step size $\triangle t$ is adopted. The discretized parameterized nonlinear system at $t_k = k\Delta t$ is written as

$$\mathcal{F}^k(\mathcal{X}^k; \text{Pat}) = 0, \tag{4}$$

where the unknown vector $\mathcal{X}^k$ is the approximation of $\mathcal{X}(t_k)$.

3 Nonlinear elimination preconditioned inexact Newton

To solve the nonlinear systems (4) with different parameters, we often use the traditional inexact Newton method combined with a preconditioned Krylov subspace method for the Jacobian problem [1]. The method is usually efficient for normal arteries, but for abnormal arteries including stenosis and aneurysm, the convergence often becomes more difficult; see Fig. 3. The main reason is that some highly nonlinear components of the residual appear near the stenotic and sometime the inlet regions. In this section, we focus on a learning-based nonlinear elimination preconditioned inexact Newton introduced in [7] to improve the convergence of the inexact Newton method. Consider a general parameterized nonlinear algebraic system

$$F(X) \equiv F(X; \text{Pat}) = 0, \tag{5}$$

for any Pat $\in D$ which is a given parameter space and the nonlinear operator $F : \mathbb{R}^n \to \mathbb{R}^n$ may involve unbalanced nonlinearities. In general, the nonlinear elimination technique attempts to remove the local high nonlinearity by solving a suitable low-dimensional subspace nonlinear system

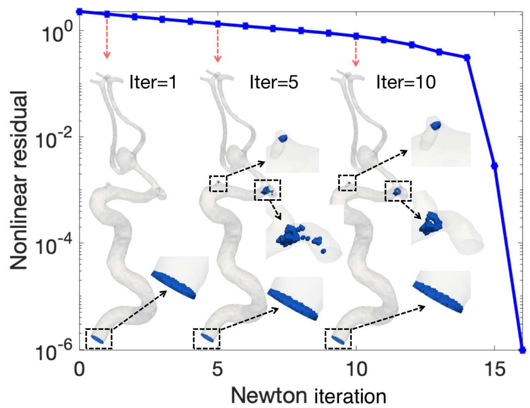

Fig. 3 The history of nonlinear residuals with the location with large residuals.

$$F_d(Y_d) \equiv R_d F(X^0 + E_d Y_d) = 0. \tag{6}$$

with $d \ll n$ which is a small integer representing the dimension of the slow subspace, where X^0 represents a known global initial guess, $R_d : \mathbb{R}^n \to \mathbb{R}^d$ is a restriction matrix whose rows span a residual subspace of dimension d and $E_d : \mathbb{R}^d \to \mathbb{R}^n$ is an extension matrix whose columns span an approximate solution subspace. Then the Jacobian matrix J_d of F_d at $Y_d \in X^0 + \text{span}\{E_d\}$ satisfies

$$J_d(Y_d) = R_d J(X^0 + E_d Y_d) E_d, \tag{7}$$

where J is the Jacobian matrix of F. Following [7], define F^i and X^i $(i = 0, \ldots, s-1)$ as the residuals and approximate solutions, and then the restriction and extension matrices are constructed based on the mean-shifted residuals and approximate solutions, denoted by $\{F_c^i\}_{i=0}^{s-1}$ and $\{X_c^i\}_{i=0}^{s-1}$, where $F_c^i = F^i - \sum_{i=0}^{s-1} F^i/s$ and $X_c^i = X^i - \sum_{i=0}^{s-1} X^i/s$. Specifically, denote $\mathbb{F}_c = [F_c^0, \ldots, F_c^{s-1}]$ and $\mathbb{X}_c = [X_c^0, \ldots, X_c^{s-1}]$, using the singular value decomposition (SVD)

$$\mathbb{F}_c = U_F \Sigma_F V_F^T, \quad \mathbb{X}_c = U_X \Sigma_X V_X^T, \tag{8}$$

where Σ_F (Σ_X) is a diagonal matrix with singular values, and U_F (U_X) is an orthogonal matrix consisting of eigenvectors, we obtain the subspace matrices by

$$R_d = [u_F^1, \ldots, u_F^d]^T, \quad E_d = [u_X^1, \ldots, u_X^d], \tag{9}$$

where $\{u_F^i\}_{i=1}^d$ and $\{u_X^i\}_{i=1}^d$ are the first d columns of U_F and U_X, respectively.

Based on the above discussion, we now introduce a learning-based method for the parameterized nonlinear system (5) for any Pat $\in D$, including a training phase and a testing phase.

Training phase $\text{Pat}_0 \longrightarrow (s, d, R_d, E_d)$.

Input: select a typical parameter set $\text{Pat}_0 \in D$.
Data collection: obtain the residuals $\{F^i\}_{i=0}^{s-1}$ and approximate solutions $\{X^i\}_{i=0}^{s-1}$ by solving the nonlinear system (5) with the specific parameter Pat_0 by the inexact Newton method.
Data analysis: try different values of s and d, and obtain U_F and U_X by (8) such that $\text{PIN}^{\mathcal{L}}$ [7] converges well for Pat_0.
Output: two parameters s, d, and the subspace matrices R_d and E_d by (9).

Testing phase
Input: pick any $\text{Pat} \in D$ and two subspace matrices R_d and E_d from the Training phase.
Subspace solution: solve the subspace nonlinear system (6) using the exact Newton method to find the subspace solution Y_d^*, where the subspace Jacobian matrix J_d is calculated by (7) in each subspace Newton iteration.
Global solution: the nonlinear system (5) with Pat is solved by the inexact Newton method with the new global initial guess $Y^0 = X^0 + E_d Y_d^*$ to obtain the global solution.

In the above algorithm, the parameter s is determined by the number of Newton iterations required to solve the nonlinear system (5) for Pat_0, while the parameter d can be controlled by the decomposition (8) using a suitable energy threshold. For Pat_0, the singular value decomposition indicates that the solution of the subspace nonlinear system (6) with a small d closely approximates the solution of the global nonlinear system (5). This approximation enables rapid convergence of (5) when the subspace solution is used as the initial guess.

4 Numerical experiments

In this section, we provide some numerical experiments to illustrate the performance and robustness of the learning-based nonlinear elimination method in the simulation of pathological blood flows under various situations. We consider the patient-specific artery shown in Fig. 1. An unstructured mesh with 246647 mesh points and the time step $\Delta t = 0.005$ s are used for the discretization. The nonlinear systems are solved by a Newton-Krylov-Schwarz method [6]. In the subspace nonlinear system, the relative tolerance is set as $rtol_{loc} = 10^{-3}$. We obtain the training residual and approximate solution vectors using parameter set $\text{Pat}_0 = \{0.035, 1.06, 56, 60, 125, 74\}$ using the traditional inexact Newton method.

4.1 The training phase

We first consider the situation $\text{Pat} = \text{Pat}_0$. In the left of Fig. 4, we show the residual histories of the subspace nonlinear operator F_d and the global operator F, and the global residual is reduced to a magnitude of 10^{-2} after four subspace Newton iterations. In the right of Fig. 4, we can see that the residual of the new method declines rapidly compared with the traditional inexact Newton method. In Fig. 5, we show the distributions of the residuals at different Newton steps for the inexact Newton method (top) and the learning-based method (bottom). The first two figures list the distributions at the initial and tenth Newton steps, and the major residuals remains in the inlet region and part of stenotic regions after ten Newton iterations. The last two figures show the results at the first and third subspace Newton steps, and we can observe that after three subspace Newton iterations, the residuals are almost eliminated. Further in Table 1, we study the impact of different s (the number of training vectors) and d (the number of the principal components) on the new method. The larger the value of d, the smaller the residual obtained by the subspace Newton iterations. When some of residual and approximate solution vectors are used, we can observe that the more training vectors we use, the fewer global inexact Newton iteration is needed.

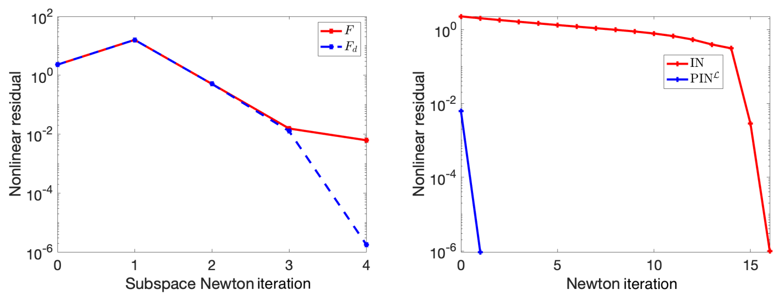

Fig. 4 The first case Pat = Pat_0 with d = 5. Left: comparison of the global residual F and subspace residual F_d in the subspace Newton iterations. Right: residual histories of the inexact Newton (IN) method and learning-based preconditioned inexact Newton method ($\mathrm{PIN}^{\mathcal{L}}$) .

Table 1 Influence of s and d on the learning-based method for Pat = Pat_0, where parentheses denote the initial and final nonlinear residuals in the subspace Newton iterations.

s	d	Newton(loc)	Newton(glo)	GMRES(glo)
17	3	4 (2.30, 0.11)	1	65.00
17	5	4 (2.30, 0.006)	1	62.00
17	7	4 (2.30, 0.005)	1	63.00
3	3	4 (2.30, 2.04)	5	82.60
5	5	4 (2.30, 1.72)	4	109.75
7	7	3 (2.30, 0.88)	3	145.33

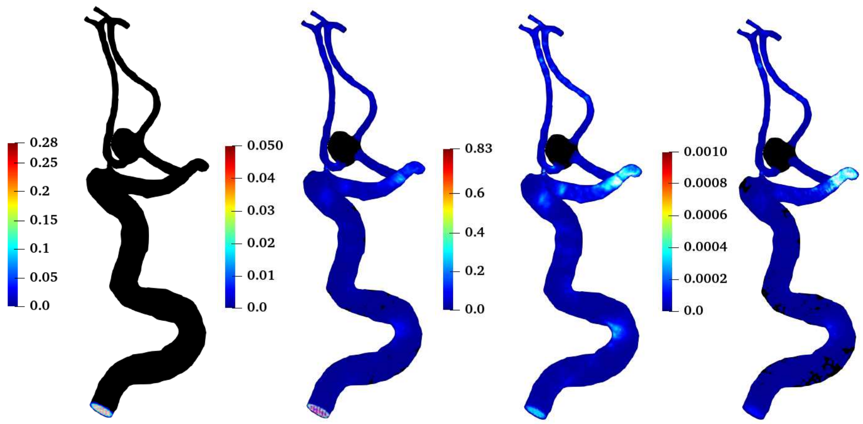

Fig. 5 Distributions of residual magnitude associated with the velocity field for the inexact Newton method (the first two figures) and the learning-based preconditioned inexact Newton method (the last two figures). From left to right: the initial and tenth Newton steps, the first and third subspace Newton steps.

4.2 The testing phase

In this subsection, we focus on the performance of the learning-based method for different parameters sets. In Table 2, we show the number of iterations with different values of viscosity, density, inflow velocity, heart rate, and pressures. We can see that the learning-based method is available for these changes. Besides, a phenomenon that the residual becomes large after the subspace Newton iterations is observed. In fact, in this case $\text{Pat} \neq \text{Pat}_0$, the discretized nonlinear operator $F(\cdot, \text{Pat})$ does not match $F(\cdot, \text{Pat}_0)$, which means that the small residual in the complementary of span $\{R_d\}$ is no longer guaranteed. Fortunately, such a phenomenon does not affect the effectiveness of the method as the strong nonlinear residual in the subspace is eliminated.

Table 2 Performance of the learning-based method for $\text{Pat} \neq \text{Pat}_0$, where parentheses denote the initial and final nonlinear residuals in the subspace Newton iterations.

Patient parameter	d	Newton(loc)	Newton(glo)	GMRES(glo)
$\mu = 0.08$	3	3 (3.43, 7.93)	3	48.33
$\mu = 0.1$	3	3 (3.95, 11.41)	3	42.67
$\rho = 1.12$	3	4 (2.36, 2.58)	3	127.67
$u_S = 66$	3	4 (3.06, 85.08)	4	199.25
$r_C = 200$	3	4 (2.78, 1.92)	3	274.67
$p_S = 200$	2	4 (2.30, 131.20)	4	178.50
$p_D = 60$	3	4 (2.30, 41.15)	3	84.33

5 Conclusion

We introduce a learning-based nonlinear elimination method for the simulation of blood flows in abnormal arteries with different inflow rate, heart rate, viscosity, density, systolic pressure, and diastolic pressure. To improve the slow convergence the traditional inexact Newton method, we extract the principal subspace using the PCA method in the nonlinear residual sequences and then eliminate them by solving the corresponding subspace nonlinear system. As the slow-convergence phenomena for different parameters are similar, such a method is very efficient when the parameters change within a suitable space.

References

1. Cai, X.C., Gropp, W.D., Keyes, D.E., Melvin, R.G., Young, D.P.: Parallel Newton-Krylov-Schwarz algorithms for the transonic full potential equation. SIAM J. Sci. Comput. **19**(1), 246–265 (1998)
2. Cai, X.C., Li, X.: Inexact Newton methods with restricted additive Schwarz based nonlinear elimination for problems with high local nonlinearity. SIAM J. Sci. Comput. **33**(2), 746–762 (2011)
3. Cebral, J.R., Castro, M.A., Burgess, J.E., Pergolizzi, R.S., Sheridan, M.J., Putman, C.M.: Characterization of cerebral aneurysms for assessing risk of rupture by using patient-specific computational hemodynamics models. Am. J. Neuroradiol. **26**(10), 2550–2559 (2005)
4. Chen, R., Wu, B., Cheng, Z., Shiu, W.S., Liu, J., Liu, L., Wang, Y., Wang, X., Cai, X.C.: A parallel non-nested two-level domain decomposition method for simulating blood flows in cerebral artery of stroke patient. Int. J. Numer. Methods Biomed. Eng. **36**(11), e3392, 20 (2020)
5. Huang, J., Yang, C., Cai, X.C.: A nonlinearly preconditioned inexact Newton algorithm for steady state lattice Boltzmann equations. SIAM J. Sci. Comput. **38**(3), A1701–A1724 (2016)
6. Liu, Y., Qi, F., Cai, X.C.: An aneurysm-specific preconditioning technique for the acceleration of Newton-Krylov method with application in the simulation of blood flows. Int. J. Numer. Methods Biomed. Eng. **39**(12), e3771 (2023)
7. Luo, L., Cai, X.C.: PIN$^{\mathcal{L}}$: Preconditioned inexact Newton with learning capability for nonlinear system of equations. SIAM J. Sci. Comput. **45**(2), A849–A871 (2023)
8. Luo, L., Shiu, W.S., Chen, R., Cai, X.C.: A nonlinear elimination preconditioned inexact Newton method for blood flow problems in human artery with stenosis. J. Comput. Phys. **399**, 108926 (2019)
9. Quarteroni, A., Manzoni, A., Vergara, C.: The cardiovascular system: mathematical modelling, numerical algorithms and clinical applications. Acta Numer. **26**, 365–590 (2017)
10. Tang, B.T., Fonte, T.A., Chan, F.P., Tsao, P.S., Feinstein, J.A., Taylor, C.A.: Three-dimensional hemodynamics in the human pulmonary arteries under resting and exercise conditions. Ann. Biomed. Eng. **39**, 347–358 (2011)
11. Yang, H., Hwang, F.N., Cai, X.C.: Nonlinear preconditioning techniques for full-space Lagrange–Newton solution of PDE-constrained optimization problems. SIAM J. Sci. Comput. **38**(5), A2756–A2778 (2016)